

Coupled Field Circuit Analysis for Characteristic Comparison in Barrier Type Switched Reluctance Motor

J.Y. Lee*, G.H. Lee*, J.P. Hong*, J. Hur** and Y.K. Kim***

Abstract - This paper deals with two kinds of novel shape switched reluctance motors (SRM) with magnetic barriers in order to improve operating performances of prototype. The magnetic barriers make rotor poles more saturated, and consequently inductance profiles are distorted. The changed inductance affects input current shape and eventually torque characteristics. In order to analyze the complicated flux pattern of the SRM with magnetic barriers and its terminal characteristics simultaneously, coupled field circuit modeling method is used. The finite element method is used to model the nonlinear magnetic field, and coupled to the circuit model of the SRM overall system. After experimental results are presented to prove the accuracy of the method, the several analysis results are compared, and the improved rotor shape is presented.

Keywords: Coupled Field Circuit Analysis, Finite Element Method, Magnetic Barrier, Switched Reluctance Motor

1. Introduction

In reluctance motors, design of magnetic barrier or salient pole is important portion for overall design process because the number or configuration of the magnetic barrier and pole affects inductance profiles, and that can change operating performance. Most papers about reluctance motor design, however, consider only the magnetic barrier or salient pole to improve the characteristics.

This paper deals with two novel shape switched reluctance motors (SRM) with inserted magnetic flux barriers in order to improve operating performances of prototype. In comparison with conventional SRM, the SRM with inserted magnetic flux barrier is easily saturated when the rotor moves towards the alignment with the stator. Consequently inductance profiles are distorted, and the changed inductance affects input current shape and eventually torque characteristics.

In order to analyze the complicated flux pattern of the three SRM, the prototype and the two proposed motors with magnet barriers, and its terminal characteristics simultaneously, coupled field circuit modeling method is used [1],[2]. The 2-dimensional finite element method (2D FEM) is used to model the nonlinear magnetic field of the SRM, and experimental equation is added to consider the end-coil effect such as fringing effect. The FEM results are coupled to the circuit model of the overall system. After experimental results are presented to prove the accuracy of the

method, the several analysis results of the three SRM are compared, and the improved rotor is presented.

2. Analysis Model

The rotors of prototype and barrier-type SRM which have inserted magnetic flux barrier are shown in Fig. 1. The magnetic flux barrier is divided into two parts, pole barrier and link barrier. If the rotor has both pole barrier and link barrier, the motor is called BSRM, and if it has only pole barrier, the motor is called PBSRM in this paper. For BSRM, the magnetic barriers have been optimized by response surface methodology to increase average torque and reduce torque ripple[1]. The PBSRM has partial magnetic barriers of BSRM. The barrier shape of PBSRM is designed by considering magnetic flux paths of general SRM so that main flux path directly crosses the rotor to each counter part pole when a switch is turned on and off by phases. The three models' wire-cut segments are shown in Fig. 2.

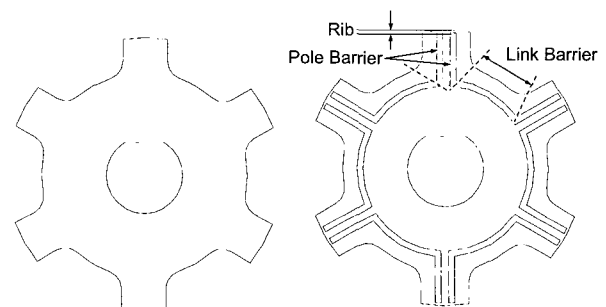


Fig. 1 Configurations of prototype and barrier type rotors

* Department of Electrical Engineering, Changwon National University, #9 Sarimdong, Changwon, Gyeongnam, Korea (jyecad@korea.com)

** Precision Machinery Research Center of Korea Electronic Technology Institute, Gyeonggi-do, Korea (jinhur@keti.re.kr)

*** Samsung Electronics Co., Ltd. (ensigma@korea.com)

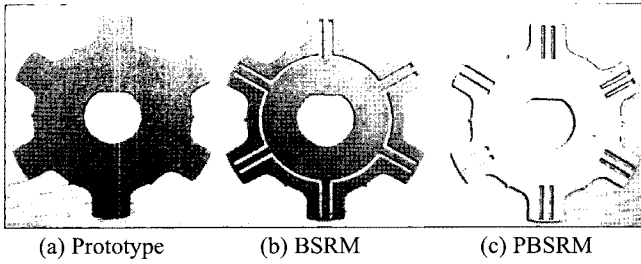


Fig. 2 SRM configurations in comparison

3. Analysis Method

3.1 Coupled Field Circuit Analysis

For the reliable characteristics analysis of the three models, not only complicated flux pattern of them, but also its terminal characteristics should be considered. To solve terminal equations and the flux equations at the same time, the coupled field circuit modeling method is effective [2].

The magnetic field of the SRM is governed by the 2D Poisson equation as follows.

$$\frac{\partial}{\partial x} \left(v \frac{\partial A_z}{\partial x} \right) + \frac{\partial}{\partial y} \left(v \frac{\partial A_z}{\partial y} \right) = -J_0 \quad (1)$$

By solving this magnetostatic equation, the internal distribution of the magnetic field can be obtained. However, the winding currents which determine the current density, J_0 , must be known for solving the equations.

The terminal voltage equations of the SRM can be easily written according to the circuit configuration of the system. For four-phase stator windings, the voltage equation is as follows.

$$v_{abcd} = r i_{abcd} + \frac{d\lambda_{abcd}}{dt} \quad (2)$$

where $v_{abcd} = (v_a, v_b, v_c, v_d)^T$ are the terminal voltages across the stator windings; $i_{abcd} = (i_a, i_b, i_c, i_d)^T$ are the phase currents of the stator windings; $\lambda_{abcd} = (\lambda_a, \lambda_b, \lambda_c, \lambda_d)^T$ are the flux linkages of the stator windings; and r is the winding resistance of the stator. 'T' indicates a transposed matrix. To find terminal current, the flux linkage variation as a function of time must be known.

Between (1) and (2), there are relations of variables. Current vector, i_{abcd} in (2) is related to the current density J_0 in (1), and flux linkage vector, λ_{abcd} , is related to the vector potential A_z . In the coupled modeling method, the (1) and (2) are to be solved simultaneously by numerical iterations. A matrix of equations contained in (1) is discretized into elemental form over the entire SRM cross-

section as usual in finite element analysis for magnetostatic field analysis.

To discretize (2), one critical problem is to discretize the time derivatives, $d\lambda_{abcd}/dt$. The time derivative is replaced by the backward difference. That is as follows.

$$\begin{aligned} \frac{d\lambda_{abcd}}{dt} &= \frac{\Delta\theta}{\Delta t} \frac{d\lambda_{abcd}}{d\theta} \\ &= w_r \frac{\lambda_{abcd}(\theta, t_\theta) - \lambda_{abcd}(\theta - \Delta\theta, t_{\theta - \Delta\theta})}{\Delta\theta} \end{aligned} \quad (3)$$

where, $w_r = \Delta\theta/\Delta t$. As indicated clearly by (3), the time derivative terms are properly discretized. Then, the global equation set containing (1) and (3) can be obtained and solved simultaneously, provided that the terminal voltages V_{abcd} and detailed geometry of the SRM are given.

Fig. 3 shows the computation flow chart used for the coupled field circuit analysis modeling method of the SRM. Two major loops are designed in the algorithm, the inner current loop and the outer rotor position loop.

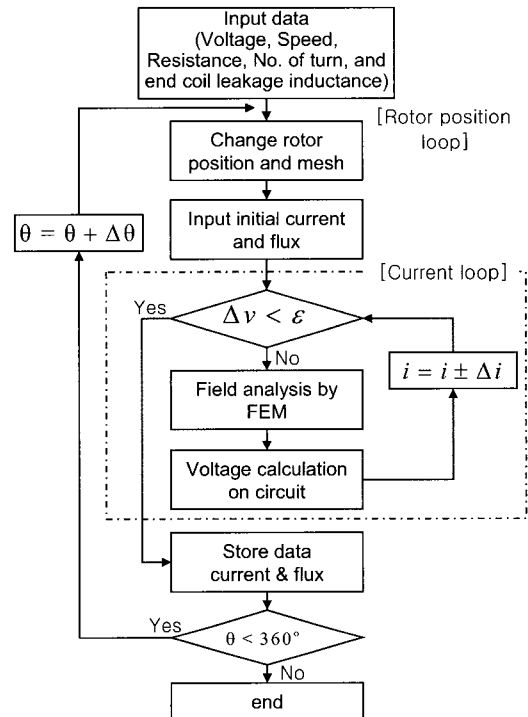


Fig. 3 Flow chart of coupled field modeling method

Note Δv , included in the inner current loop, is the difference between the actually applied voltage and the computed voltage from (2) for the current assumed. As soon as Δv falls within the predetermined error, the currents assumed converge to their true values which, in turn, determine the field vector potential of the SRM. If constant current is given to system, the current loop can be skipped except the step of field analysis by FEM in the flow chart.

3.2 End Winding Effect

By 2D FEM, the end winding effect can not be considered. In order to remedy this problem, some experimental equations can be used depending on the coil shapes [3], [4]. One example is (4), which is used for calculation of end coil inductance per phase, L_{end} , in switched reluctance motors [3].

$$L_{end} = (N_p / P_{th}) \times \mu_0 a N_{ss}^2 \ln(8a / GMD - 2) \quad (H) \quad (4)$$

where N_p is the number of turns per pole, P_{th} is the number of parallel paths in the phase winding, a is coil radius, N_{ss} is number of pole-coils in series per phase, and GMD is geometric mean distance of coil side cross-section.

4. Experimental Testing Verification

The computation procedures outlined in the flow chart are implemented and the EMF program, developed by ECAD laboratory is used serving as the major subroutine. Several analyses and experiments have been conducted on the three models. The basic specifications of the prototype are listed in Table 1.

Table 1 Specifications of Prototype

Rated Power	260 W	Torque	1.4 N-m
Input Voltage	150V	Base Speed	1800rpm
Rated Current	1.9 A	No. of Poles	8/6
Stator OD	90mm	Stack Length	95mm
Turn-on Angle	5°	Turn-off Angle	20°

4.1 Experiment at Current Operation Mode

The 2D geometry of the SRM and the equipotential lines are shown in Fig. 4. As shown in these figures, the rotor poles of BSRM are more saturated than the others because of magnetic flux barriers. This saturation affects inductance profiles as shown in Fig. 5, in which the inductance profiles are changed according to current, rotor displacement, and barrier shape. The displacement represents the rotor position. 0° denotes the position where stator pole and rotor pole are unaligned and 30° denotes the position where the rotor pole is aligned to the current excited stator pole.

In Fig. 5, the analysis data is obtained by coupled field modeling method at constant current condition for which the current loop is skipped except the step of field analysis by FEM in the flow chart, Fig. 3. It is seen that even at the same condition in current and rotor displacement, the inductance profiles are distorted by magnetic flux barrier shape.

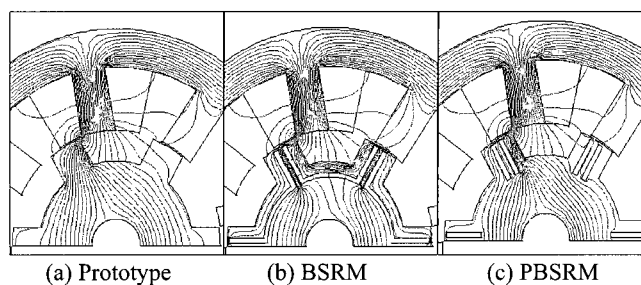


Fig. 4 Equipotential line of three models

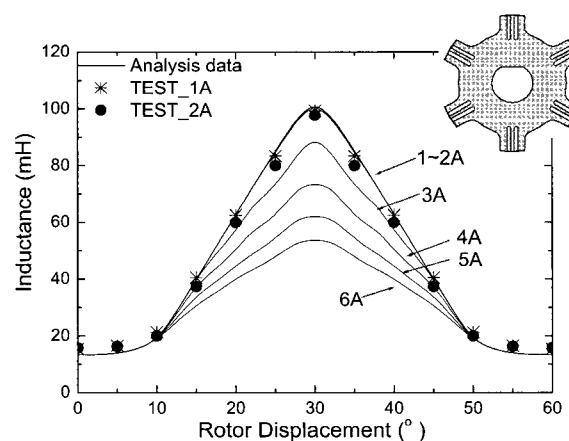
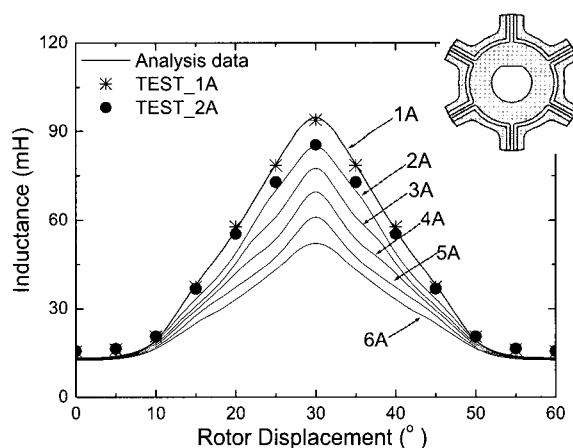
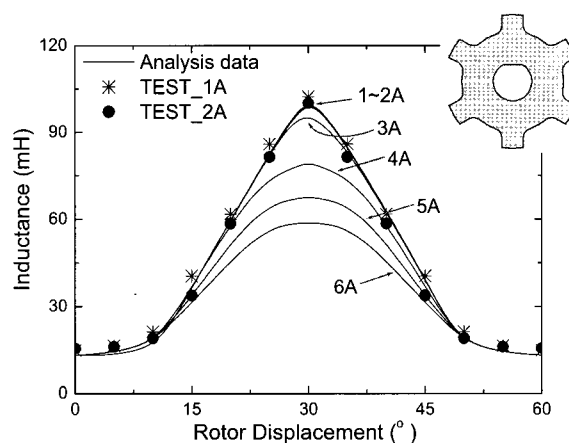


Fig. 5 Comparison of inductance profile with analysis and test data

The experimental results of these tests are obtained from a measuring method of AC power at constant current. The method used AC power, the inductance was calculated by measured voltage, V_{rms} , current, I_{rms} , and phase angle, θ using Eq. (4).

$$R = \frac{V_{rms} \cos \theta}{I_{rms}}, \quad L = \frac{V_{rms} \sin \theta}{\omega I_{rms}} = \frac{V_{rms} \sin \theta}{2\pi f I_{rms}} \quad (4)$$

where, the frequency, f , is 50Hz in the test.

The analytical and experimental inductances are in substantially agreement as shown in Fig. 5. The results give reliance on the input data, FEM as field analysis method, and consequently the rotor position loop in the flow chart, Fig. 3.

4.2 Experiment at Voltage Operation Mode

Fig. 6 shows the comparison of calculated and measured currents of prototype. The calculated result is obtained by coupled field modeling method at 80V switch turn-on voltage, 150V turn-off voltage, and 800 rpm speed. The measured current is obtained by computer controlled DSP driver under the same condition. By this comparison, it is noted that the simulation results shows a good agreement with the experimental results. It is clear that the current waveform predicted by the coupled field circuit modeling method is in a very good agreement with that from the testing.

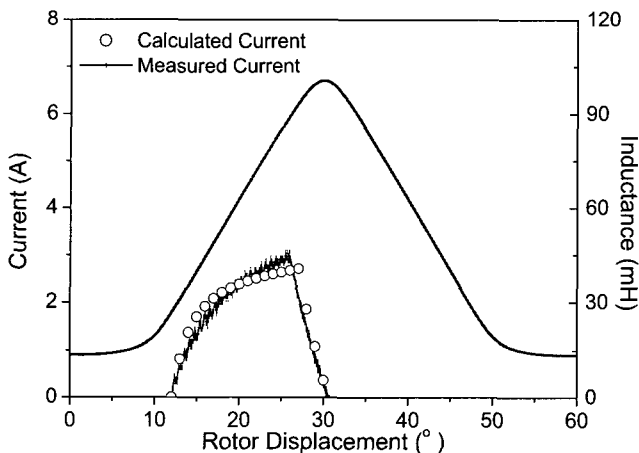


Fig. 6 Comparison of calculated and measured currents of prototype

5. Results of Theoretical Analysis

Fig. 7 shows the comparison of analysis results for three models by the coupled field circuit modeling method. The analysis condition is the same as rated condition of prototype as mentioned in table 1.

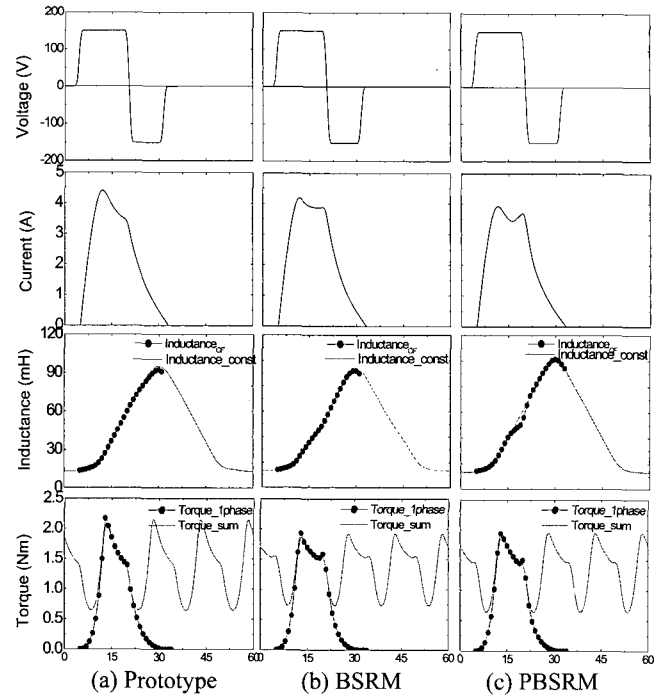


Fig. 7 Comparison of characteristics at 1800rpm

It is noted that although the input voltage maintained constant for 15° , rotor position, the phase current fluctuates over 1A after reaching its peak value at about 12° . Furthermore, the peak current does not correspond to the instant when the maximum flux linkage occurs. After the transistor is turned off, the phase current takes a sit of time to decay. Despite of same operating condition, the current fluctuations are different because of distorted inductance due to the magnetic barriers. When the rotor moves towards the alignment with the stator, the rotor poles start to be saturated, and inductance profile of prototype become curved. However, the inductance profiles of BSRM become so straighter under saturation condition that the current can keep the plate top current shape during switch turn-on period. For PBSRM, the inductance profile is also curved, but its direction is opposite to that of prototype. It causes different current fluctuating shape.

Consequently the torque characteristics are different from each other because of the different current and inductance profiles. According to this comparison, BSRM has less torque ripple than that of prototype at rated speed 1800 rpm.

Fig. 8 shows the torque characteristics of the three models according to speed variation 1000-2000 rpm. The input conditions such as input voltage and switch turn-on and off angle are same as in Table I. It is noticeable that even though the output power is identical to each other at high speed, the torque ripples are quite different. The difference of torque ripple between prototype and barrier type SRM, PBSRM and BSRM, is increased as speed increases. Therefore, at high speed the BSRM can be a good model to reduce torque ripple of SRM.

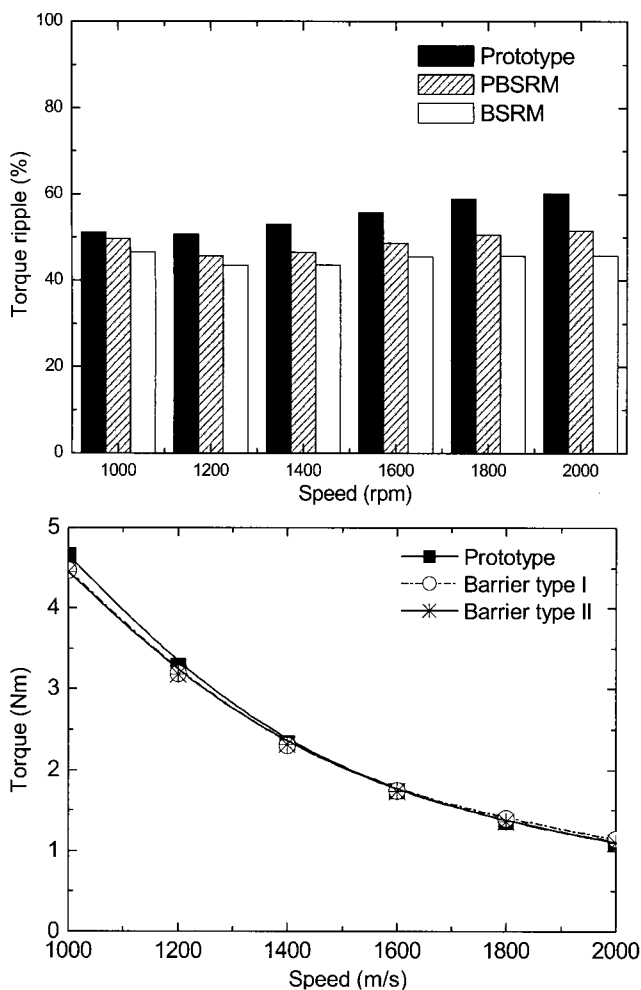


Fig. 8 Torque characteristics according to speed variation

6. Conclusions

This paper dealt with two SRM with inserted magnetic flux barriers in order to improve operating performances of prototype, and the coupled field circuit modeling method was used to reliably evaluate the characteristics of the motors.

By experimental results, not only validation of the FEM and the coupled field circuit analysis method, but also effect of magnetic flux barrier due to changed inductance profiles is evaluated. And the results obtained by the coupled field circuit analysis method show that the SRM with magnetic flux barriers can reduce torque ripple.

In design of SRM considering control, the magnetic flux barrier can be the important factor, and these results can be used useful references.

References

- [1] Young-Kyoun Kim, Ji-young Lee, Jung-Pyo Hong, and Jin Hur, "Optimization of Barrier type SRMs with Response Surface Methodology Combined with Moving Least Square Method," International Symposium on Electromagnetic Fields in Electrical Engineering (ISEF2003), vol.2/2, pp659-664, September 18-20, 2003, Maribor, Slovenia.
- [2] Longya Xu and Eric Ruckstadter, "Direct Modeling of Switched Reluctance Machine by Coupled Field-Circuit Method," IEEE Trans. on Energy Conversion, vol. 10, No. 3, pp446-454, September, 1995
- [3] TJE Miller, *SPEED Consortium PC-SRD version7.0 Uwer's Manual*, University of Glasgow, June 1999
- [4] Frederick W. Grover, *Inductance Calculations*, D. Van Nostrand Company, Inc.